USING GEOGRAPHIC OBJECT-BASED IMAGE ANALYSIS (GEOBIA) FOR URBAN LAND COVER MAPPING AND SETTLEMENT DENSITY ASSESSMENT

C. Berger [a, *], M. Voltersen [a], S. Hese [a], I. Walde [a], C. Schmullius [a]

[a] Department for Earth Observation, Friedrich-Schiller-University Jena, Löbdergraben 32, D–07743 Jena, Germany – (christian.berger, michael.voltersen, soeren.hese, irene.walde, c.schmullius)@uni-jena.de

KEY WORDS: Object-based, Urban, Land Cover, Classification, Settlement Density, Analysis, Quickbird, LiDAR

ABSTRACT:

This study presents a geographic object-based image analysis (GEOBIA) workflow to produce a high-resolution urban land cover map and settlement density information for the city of Rostock, Germany. For this purpose, multi-spectral Quickbird imagery and an object height model derived from light detection and ranging (LiDAR) data are used. In a first step, the GEOBIA approach is employed to infer six basic urban land cover classes. To foster the reproducibility and the spatio-temporal transferability of the ruleset, emphasis is put on the compilation of simple but efficient class descriptions. In a second step, the intensity of urban development is assessed by means of a new urban density (UD) metric. UD is calculated for each individual building in the land cover map and within a predefined area of interest (AOI) around the centroid of the respective building. UD maps and statistics are obtained by a logical combination of four input parameters describing settlement aggregation, the degree of soil sealing, the abundance of urban vegetation and the intensity of vertical development within the AOI. Hence, each of those inputs evaluates a different aspect of the urban environment. The study results show that the object-based classification paradigm is well-suited for an accurate and consistent extraction of urban land cover information (Overall Accuracy: 91.3 %; Kappa Index: 0.89). The findings of the UD analyses highlight the plausibility and qualification of the proposed metric as a measure to assess human settlement density and its distinct spatial patterns for different types of urban land use. By taking into account horizontal and vertical characteristics of a city, an integrated and more holistic view on settlement density in all three spatial dimensions is enabled.

1. INTRODUCTION

Human settlements are complex and dynamic systems having diverse and profound impacts on environmental factors and processes (Scalenghe & Marsan, 2009). Due to the isolation of the land surface by impervious materials, soil permeability in urban areas is significantly reduced. As a result, groundwater tables are forced to decrease while, at the same time, surface runoff increases (Niemczynowicz, 1999; Tang et al., 2005). The hydrological cycle is therefore highly affected by the presence and intensity of urban development. Settlements also influence energy and heat fluxes between soil and atmosphere. Especially during longer periods of heat stress, a phenomenon called urban heat island (UHI) is observable (Oke, 1973; Gluch et al., 2006). Because construction materials store thermal energy longer than natural cover types, cities often feature higher air temperatures than their hinterland at night time. The UHI effect is amplified by a decrease of reflected solar radiation that is caused by the low albedo of roof tops and asphalted surfaces (Scalenghe & Marsan, 2009). The abundance of building objects adds a third dimension to the ecological relationships found in urban areas. Since height, orientation, arrangement and density of buildings alter, e.g., micro-climatic factors and conditions such as wind speed and ventilation paths within cities (Klysik & Fortuniak, 1999; Huizhi et al., 2002), urban environmental variables are subject to both horizontal and vertical properties of settlements. Hence, urban environmental studies should rely on information sources that account not only for the horizontal dimension, but also for the vertical dimension to enable an integrated and more holistic assessment of the 'builtscape' (Dell'Acqua, 2009).

This work aims at providing one such information layer. We present an object-based feature extraction workflow to produce a high-resolution urban land cover map and settlement density information for the city of Rostock, Germany. For this purpose, use is being made of multi-spectral Quickbird imagery and an object height model derived from light detection and ranging (LiDAR) data. Particular emphasis is put on the development of a metric to assess urban density (UD) by taking into account both the horizontal *and* vertical characteristics of a city. The paper is structured as follows. In the upcoming section, the data and methods used to achieve the above goal are presented. This section is followed by a description and discussion of the study results. Finally, the findings of this investigation are concluded and an outlook with regard to future research needs is provided.

2. MATERIALS & METHODS

The overall workflow of this study consists of three consecutive steps: (1) data preparation, (2) extraction of urban land cover information and (3) derivation of UD maps and statistics. In the following, each of these steps is described in more detail.

2.1 Data basis & data preparation

The data basis used in this study comprises a cloud-free multi-spectral Quickbird scene and a normalised digital surface model (nDSM) derived from airborne LiDAR data. Both datasets have been acquired over the city of Rostock, Germany. An overview of the datasets is compiled in Table 1 and Table 2.

* Corresponding author at Department for Earth Observation, Friedrich-Schiller-University Jena, Löbdergraben 32, D–07743 Jena, Germany. Tel.: +49(0)3641 948974; fax: +49(0)3641 948882. E-mail address: christian.berger@uni-jena.de (C. Berger).

Table 1. The Quickbird dataset used in this study.

	Quickbird
Acquisition date	2009-09-19, 12:21 CET
Spectral bands	Blue, Green, Red, Near-Infrared (NIR), Panchromatic (PAN)
Spatial resolution	0.6 m (PAN), 2.4 m (multispectral)
Radiom. resolution	(provided in) 16 bits per pixel

Preprocessing of the Quickbird imagery comprises three steps. First, to correct the scene for atmospheric effects and to convert the 16 bit digital numbers to reflectance values, a radiometric normalisation is applied to the data using ATCOR-2 (Richter et al., 2006). Second, to obtain a multi-spectral scene at the spatial resolution of the panchromatic band, image fusion is performed at pixel level using the high-pass filter (HPF) resolution merge (Gangkofner et al., 2008). Third, to spatially match the multi-spectral scene to the LiDAR dataset, orthorectification is done using more than 250 well-distributed ground control points and a digital elevation model (DEM) covering the area.

Table 2. The LiDAR dataset used in this study.

	LiDAR
Acquisition period	2006-03-01 to 2006-09-30
Image bands	nDSM, DSM, DEM
Spatial resolution	2 m (derived from 2 shots per m²)
Radiom. resolution	32 bits per pixel

The nDSM is derived from airborne LiDAR (Light Detection and Ranging) data using LAStools (Isenburg et al., 2011). First, a digital surface model (DSM) is generated using non-ground LiDAR points only. Second, the DEM is then subtracted from the DSM to obtain the nDSM. This information layer contains the height of urban objects relative to the ground.

With respect to the subsequent urban land cover classification, additional information layers are derived from the input data. Brightness indicates the average reflectance of all bands in a multi-spectral dataset. It is defined as

$$\text{Brightness} = \frac{\rho(\text{Blue}) + \rho(\text{Green}) + \rho(\text{Red}) + \rho(\text{NIR})}{4} \tag{1}$$

where ρ is the reflectance of the respective Quickbird channels (cf. Table 1). Brightness ranges between 0 and 10000 (i.e., 0 and 100.00 % reflectance). Increased brightness values indicate consistently high reflectance values among all spectral bands under consideration. As a measure of the abundance and vigour of vegetation at the land surface, the Normalized Difference Vegetation Index (NDVI) is defined as

$$\text{NDVI} = \frac{\rho(\text{NIR}) - \rho(\text{Red})}{\rho(\text{NIR}) + \rho(\text{Red})} \tag{2}$$

where ρ is the reflectance of the respective Quickbird channels (cf. Table 1). NDVI ranges between –1 and +1. Higher NDVI values indicate greater amounts of vigorous vegetation (Tucker, 1979). Finally, slope (in percent) is derived from the nDSM following Zevenbergen & Thorne (1987). This information is useful for identifying transitions between flat areas and elevated objects such as buildings (Priestnall et al., 2000). Higher slope values indicate steeper transitions.

2.2 Extraction of urban land cover information

As it is required for the derivation of UD, high-resolution urban land cover information is extracted from the input data. The six target classes are buildings, impervious, trees, grass/shrubs, bare soil and water bodies. With regard to the overall goal of this study, particular focus is put on the accurate delineation of buildings and impervious areas. For this purpose, a geographic object-based image analysis (GEOBIA) approach (Blaschke & Strobl, 2001; Benz et al., 2004; Blaschke et al., 2008; Blaschke, 2010) is employed. First, a series of segmentation algorithms is applied to the input data to create image objects that correspond to a predefined homogeneity criterion. As a result, larger image objects are obtained for homogeneous regions such as water bodies and bare soil areas, whereas smaller image objects are obtained for heterogeneous regions such as densely built-up areas. After the initial segmentation, a rule-based classification of image objects is performed following the scheme depicted in Figure 1. To foster the reproducibility and the spatio-temporal transferability of the ruleset, the compilation of complex class descriptions is avoided.

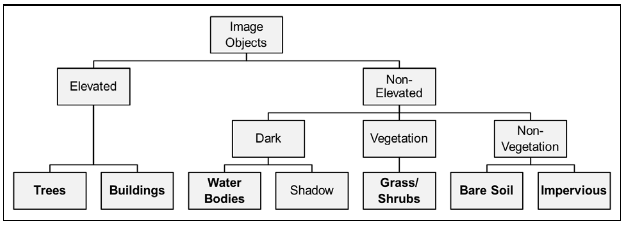

Figure 1. The urban land cover classification scheme applied to the image objects. The six target classes are displayed in bold.

Image segments are first divided into elevated and non-elevated objects using the LiDAR nDSM. An object height of 2 m serves as separation threshold. The threshold is chosen to enable the differentiation between small, but elevated image objects such as allotment garden cottages and pseudo-elevated image objects such as large vehicles (cf.Yu et al., 2010). Subsequently, image brightness, NDVI as well as nDSM slope are used to classify elevated image objects as trees or buildings (cf. Priestnall et al., 2000). In a next step, non-elevated objects are labelled as 'dark' if a predefined brightness criterion is satisfied. Since dark objects can be assigned to water bodies or shadowed areas, their size, relative border to building or tree objects and brightness standard deviation are employed to discriminate between these classes. The underlying assumption is that water objects cover larger areas, share smaller common borders to buildings or trees and feature less brightness inhomogeneity than shadows. The distinction between vegetated and non-vegetated regions is accomplished by means of the NDVI. While vegetation objects are immediately classified as grass/shrubs, other non-vegetated areas are subdivided into bare soil and impervious surface cover employing image brightness values and their standard deviation. Afterwards, urban tree objects are reshaped to correct for the systematic underestimation of sealed areas due to tree crowns (Ramanauskas, 2009). Other reshaping algorithms are used to optimise the borders of some of the thematic image objects that have been created and classified. As the final step of the rule-based land cover classification, shadow objects are reassigned to the class they share the largest relative common border with.

To assess mapping accuracy, use is made of digital orthophotos (DOPs) and Jena Airborne Scanner (JAS) data (Georgi et al., 2005) that have been acquired over Rostock in 2009 and 2010, respectively. The spatial resolution of the datasets is 0.2 m. A random sampling design (Stehman, 2009) is chosen comprising 100 sample points per land cover class. In this way, classes with small areal coverage are equally represented in the validation scheme. The actual land cover at each sample point location is then extracted from the reference data and compared to the map. Finally, the numeric results of the comparison are transferred to an error matrix to assess overall classification accuracy, errors of commission and omission as well as the kappa coefficient of agreement (Stehman, 1997; Cohen, 1960).

2.3 Derivation of UD maps and statistics

The basic requirements for the derivation of urban density (UD) are the urban land cover map and the object height information provided by the LiDAR nDSM. Density values are calculated for each single building and within a predefined radius (Area of Interest, AOI) around the centroid of the respective building. They are the result of a logical combination of four parameters quantifying the intrinsic structure of settlements, soil sealing, urban vegetation as well as the intensity of vertical development within the AOI. Since each of the input variables evaluates a different and distinct attribute of the 'builtscape' (Dell'Acqua, 2009), the resulting information layer enables an integrated and more holistic assessment of local UD patterns.

The indices used to assess UD are building aggregation (BA), impervious surface area (ISA), inverted floor area ratio (iFAR) and vegetation fraction (VF). *BA* describes the arrangement and compactness of buildings within the AOI. It is defined as

$$BA = \frac{\left(\frac{\Sigma A_b}{A_{AOI}}\right)}{\mathrm{Median}(D_b)} - \frac{\mathrm{Median}(iFAR)}{N_b} \tag{3}$$

where A_b is the floor area covered by each building, A_{AOI} is the area of the AOI, D_b is the distance of buildings within the AOI to their nearest counterpart and N_b is the number of buildings. iFAR as an indicator of vertical sealing is described in Equation (5). For the calculation of BA, the median building distances as well as the median iFAR of all buildings within the AOI are used. BA is normalised between 0 and +1 to match its values to the range of the input parameters. The left term of the above expression is proportional to BA and increases if the building coverage ratio (BCR) (Pan et al., 2008) increases while the distances between buildings decrease within the AOI. The right term of the above expression is inversely proportional to BA and increases if the degree of vertical sealing decreases (i.e., if iFAR increases) and the number of buildings within the AOI is reduced as well. In general, UD increases with higher values of BA. *ISA* describes the degree of soil sealing within the AOI (cf. Xian & Crane, 2006). It is defined as

$$ISA = \frac{(\Sigma A_b + \Sigma A_i)}{A_{AOI}} \tag{4}$$

where A_b is the floor area covered by each building, A_i is the area covered by other impervious surfaces and A_{AOI} is the area of the AOI. ISA ranges between 0 and 1. UD increases with higher values of ISA. *iFAR* describes the ratio between the floor area and the gross floor area (GFA) of a building (cf. Yu et al., 2010). It is defined as

$$iFAR = \frac{A_b}{\Sigma A_{fl}} \tag{5}$$

where A_b is the floor area covered by a building and A_{fl} is the total area of a all floors of the same building (i.e., the GFA). iFAR ranges between 0 and 1. UD decreases with higher values of iFAR. *VF* describes the urban green area ratio within the AOI (cf. Mack et al., 2010). It is defined as

$$VF = \frac{(\Sigma A_t + \Sigma A_g)}{\Sigma A_{AOI}} \tag{6}$$

where A_t is the area covered by trees, A_g is the area covered by other urban green and A_{AOI} is the area of the AOI. VF ranges between 0 and 1. UD decreases with higher values of VF. And finally, *UD* describes the intensity of urban development with regard to horizontal and vertical settlement characteristics and is obtained by linking the above indicators as follows:

$$UD = (BA + ISA) - (iFAR + VF) \tag{7}$$

The left term of the above expression is proportional to UD and increases if BA and ISA increase as well. The right term of the above expression is inversely proportional to UD and increases if iFAR and VF increase. Given the dynamic range of its input parameters, UD ranges between –2 (very low density of urban development) and +2 (very high density of urban development).

For demonstration purposes, UD is derived for five selected test sites in the city of Rostock, Germany. Each test site represents a specific type of urban land use (e.g., after Breuste et al., 2001). The calculation of UD is based on the urban land cover map. The AOI used for the calculation of UD corresponds to a radius of 250 m around the centroid of each building object. In order to compute the area of individual floors of a single building (i.e., to calculate iFAR), a mean floor height of 2.85 m (cf. Alhaddad et al., 2008; Pan et al., 2008) is assumed. As a result, UD maps and statistics are obtained for each test site.

3. RESULTS & DISCUSSION

The results of this study are the urban land cover classification as well as UD maps and statistics. Both results are described and discussed in the following sections.

3.1 Urban land cover classification

The result of the urban land cover classification for the city of Rostock, Germany, is displayed in Figure 2. An overall area of about 260 km² has been classified as buildings, impervious, trees, grass/shrubs, bare soil and water bodies. The largest areal coverage is observed for the class grass/shrubs. Circa 37.80 % (98.24 km²) of the study area correspond to this land cover type. Trees, water bodies and bare soil cover 48.87 % (126.65 km²) of the site in equal proportions. Less than 14 % (34.71 km²) of the scene is consumed by impervious surfaces (streets, parking lots or pavements) and buildings. Besides statistical information on land cover, the classification result provides an overview of some of the distinct landscape patterns in and around the city of Rostock. Examples include large forested areas in the north-east, agricultural land use in the urban fringe and the urbanised area itself, which is concentrated along the Warnow River. The harbour of Rostock is clearly recognisable by its large industrial halls and a high percentage of sealed surfaces. The city centre, high-rise housing estates, suburbs and allotment gardens are highlighted by characteristic building shapes and arrangements.

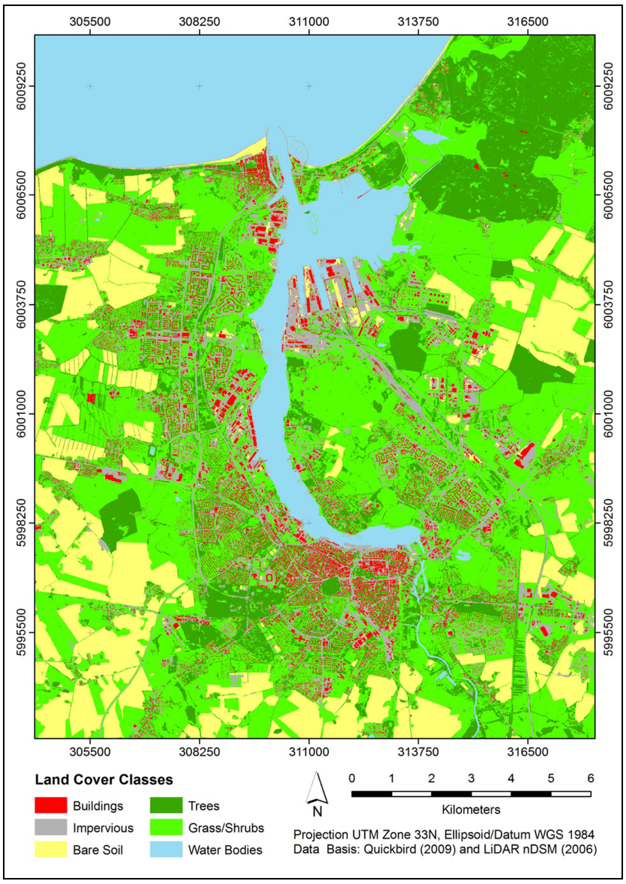

Figure 2. Urban land cover map of Rostock, Germany.

The user's (UA) and producer's accuracies (PA) for the urban land cover map are provided in Figure 3. The highest mapping accuracies are observed for water bodies and trees. All image objects classified as water are assigned to the same class within the reference dataset (100.00 %). Only few actual water bodies are misclassified as grass/shrubs (96.15 %). In rare cases, trees are mistaken for areas that are dominated by grass/shrubs and vice versa. However, the errors of commission (96.00 %) and omission (97.95 %) are still very low. 90 % of all buildings are mapped correctly by the classifier. Six out of 100 buildings are erroneously labeled as impervious and four further building objects are wrongly assigned to the class grass/shrubs. In a similar fashion, ten buildings in the urban land cover map are actually non-elevated sealed areas or bare soil. The commission error of the latter cover type is rather high (96.00 %). But on the other hand, the overall classification performance for bare soil is compromised by some errors of omission (85.71 %) that can be attributed to confusions with impervious surfaces and grass/ shrubs. In turn, the target category grass/shrubs does include a small number of image objects that, in equal shares, actually belong to the remaining cover types in the reference (84.00 %). In other cases, and as indicated above, the classifier sometimes mistakes short vegetation for trees or bare soil areas (89.36 %). Confusion is largest for the impervious class. Even though more than 89 % of the reference samples are classified correctly, only 82 % of this category in the urban land cover map is accurate. Bare soil areas are a well-known source of error in this regard (cf. Leinenkugel et al., 2011).

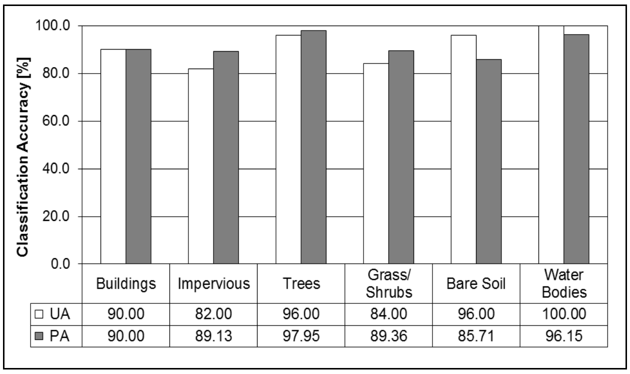

Figure 3. Accuracy of the urban land cover classification.

Apart from these minor classification errors, overall accuracy of the urban land cover map is 91.3 %. The kappa coefficient of agreement amounts to 0.89. Therefore, and according to other authors (Landis & Koch, 1977; Altman, 1991; Grouven et al., 2007), the mapping result can be considered as very good and suitable for the analysis of local UD patterns.

3.2 UD maps and statistics

Figure 4 shows UD maps for five selected land use classes. The corresponding UD statistics are compiled in Table 3. *Allotment gardens* feature the smallest UD values in the study area. They are characterised by a large percentage of vegetation (VF). The degree of horizontal (ISA) and vertical sealing (GFA) is only marginal. Thus, the median UD of allotments is only –0.93. The low standard deviation (0.18) of density is in agreement with the homogeneous spatial patterns created by the cottages within allotments. The clearly visible trend in north-south direction is due to the adjacency of the test site to an apartment block in the south of the subset. Thus, density values of up to –0.16 can be found. Single- and double family houses in *suburbs* also feature small UD values. The median density amounts to –0.67 and is comparable to buildings in allotment gardens. However, local density values for this test site range from –1.4 to –0.03 and are thus subject to an increased standard deviation (0.32). Generally speaking, the small UD in suburban areas can be explained by the low aggregation of buildings (BA), the minor degree of vertical sealing and the high percentage of vegetation cover.

Table 3. UD statistics for the five selected test sites.

	Max.	Min.	Median	Std.-Dev.
Allotment gardens	–0.16	–1.33	–0.93	0.18
Suburban area	–0.03	–1.40	–0.67	0.32
Apartment blocks	0.91	–1.23	0.14	0.44
Industrial park	1.45	–1.00	0.30	0.52
City centre	1.56	–0.17	0.99	0.37

Apartment blocks feature a median UD of 0.14. The maximum density is (0.91). Small UD values are caused by green spaces in-between blocks and adjacent allotment gardens that fall within the AOI. Especially the number of floors per building leads to larger density differences within this land use class. The median UD of *industrial parks* is slightly higher than for apartment blocks (0.30). However, the dynamic range is much broader (–1.00 to 1.45) because industrial buildings are very diverse. Accordingly, the standard deviation of UD is highest compared to all other test sites. Industrial areas are typically characterised by a high ratio of horizontal and vertical sealing. As a result, they consistently yield high UD scores. In the *city centre*, the high degree of horizontal and vertical sealing paired with the large number of buildings and the small fraction of vegetation cover leads to the largest median UD of all land use types investigated (0.99). The subset also features the building to which the highest density value was attributed to (1.56).

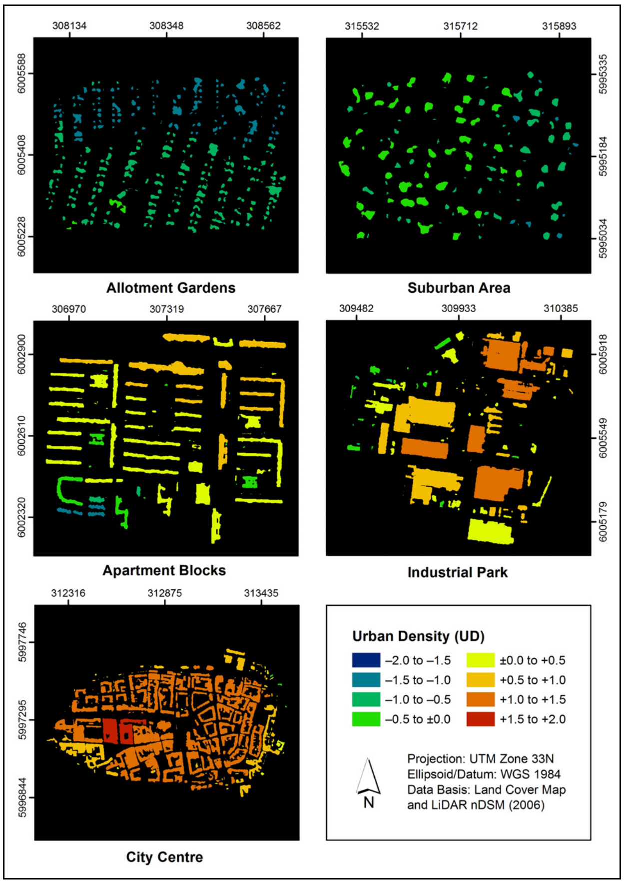

Figure 4. UD maps for the five selected test sites.

The maps and statistics that have been derived for each test site clearly demonstrate the potential of the UD metric to accurately represent the intensity of urban development for different types of land use. Moreover, a comparison between the median values found at each location suggests that UD is able to consistently reproduce the increasing degree of urban densification that can be expected in dependence of the land use class investigated. While the median UD is low for allotment gardens (–0.93), UD steadily increases with actual settlement density in suburban areas (–0.67), for apartment blocks (0.14) and industrial parks (0.30) until it reaches its peak in the city centre (0.99). It is worth noting that the density map for the entire city of Rostock does not feature the largest possible values of the UD metric (up to 2.0). On the one hand, this is in well agreement with the fact that Rostock does certainly not belong to the most concentrated urban areas in comparison to other cities in Germany, Europe or the world. On the other hand, this gives prove to the fact that UD is not prone to running into saturation when a city with comparatively moderate overall intensity of development is analysed. For this reason, it is very likely that UD values higher than those presented here can only be observed for compact urban structures in densely built-up areas. In conclusion, these findings underline the plausibility and suitability of the UD metric as a useful measure to assess density patterns in urban environments.

4. CONCLUSIONS & OUTLOOK

This study has presented a GEOBIA workflow to derive high-resolution urban land cover and settlement density information from multi-spectral Quickbird and LiDAR data. The object-based classification approach is well-suited for the consistent extraction of urban land cover and earned very high mapping accuracies (Overall Accuracy: 91.3 %; Kappa Index: 0.89). To assess the intensity of urban development, a new urban density (UD) metric was proposed that is calculated for each individual building in the land cover map and within a predefined AOI around the centroid of the respective building. UD maps and statistics were obtained by linking four parameters. Each of the used input indicators evaluates a different aspect of the urban environment as, for example, settlement structure, soil sealing, urban vegetation or the intensity of vertical development within the AOI. The results of this analysis highlight the plausibility and qualification of the proposed UD metric as a measure to assess human settlement density and its distinct spatial patterns for different types of urban land use. By taking into account horizontal *and* vertical characteristics of the 'builtscape', an integrated and more holistic view on settlement density in all three spatial dimensions is enabled.

Future research will focus on a more detailed investigation of the UD measure. Apart from further analysing its plausibility, particular emphasis will be put on (1) the added value of UD in comparison to the four input variables used to compute it, (2) the potential of UD to infer basic urban land use classes, (3) the spatio-temporal transferability of the entire GEOBIA workflow as well as (4) the consistency and comparability of UD values measured for different cities with different overall intensities of development.

ACKNOWLEDGEMENTS

This study is part of the ENVILAND2 research project, which is funded by the Space Agency of the German Aerospace Center (DLR) with financial support of the German Federal Ministry of Economics and Technology (BMWi) on the basis of legislation by the German Parliament grant no. 50EE0844–50EE0847. The authors would like to thank the land registry office Rostock for the kind provision of the LiDAR and DOP data. JAS imagery is courtesy of Jena-Optronik GmbH.

REFERENCES

Alhaddad, B.I., Roca, J., Burns, M.C. & Garcia, J., 2008. Satellite imagery and LiDAR data for efficiently describing structures and densities in residential urban land uses classification. In: *The International Archives of Photogrammetry, Remote Sensing and Spatial Information Sciences*, Beijing, China, Vol. XXXVII. Part B8, pp. 35–40.

Altman, D.G., 1991. *Practical Statistics for Medical Research*. Boca Raton, FL, Chapman & Hall/CRC Press, pp. 624.

Benz, U.C., Hofmann, P., Willhauck, G., Lingenfelder, I. & Heynen, M., 2004. Multi-resolution, object-oriented fuzzy analysis of remote sensing data for GIS-ready information. *ISPRS Journal of Photogrammetry and Remote Sensing*, 58(3–4), pp. 239–258.

Blaschke, T., 2010. Object-based image analysis for remote sensing. *ISPRS Journal of Photogrammetry and Remote Sensing*, 65(1), pp. 2–16.

Blaschke, T., Lang, S. & Hay, G., 2008. Object-based image analysis. Spatial concepts for knowledge-driven remote sensing applications. Springer, Berlin, pp. 818.

Blaschke, T. & Strobl, J., 2001. What's wrong with pixels? Some recent developments interfacing remote sensing and GIS. *GIS Zeitschrift für Geoinformationssysteme*, 14(6), 12–17.

Breuste, J., Wächter, M. & Bauer, B., 2001. Beiträge zur umwelt- und sozial-verträglichen Entwicklung von Stadtregionen, CD-Rom. Leipzig, Umweltforschungszentrum (UFZ).

Cohen, J., 1960. A coefficient of agreement for nominal scales. *Educational and Psychological Measurement,* 20(1), pp. 37–46

Dell'Acqua, F., 2009. *The role of SAR Sensors*. In: Gamba, P. & Herold, M., Eds. Global mapping of human settlement. Boca Raton, FL, CRC Press, pp. 309–319.

Gangkofner, U.G., Pradhan, P.S. & Holcomb, D.W., 2008. Optimizing the high-pass filter addition technique for image fusion. *Photogrammetric Engineering & Remote Sensing*, 74(9), pp. 1107–1118.

Georgi, C., Strognienko, R., Knuth, S. & Albe, G., 2005. JAS: *The Next Generation Digital Aerial Scanner*. In: Fritsch, D., Ed. Photogrammetric Week '05. Heidelberg: Wichmann, pp. 147–154.

Gluch, R., Quattrochi, D.A. & Luvall, J.C., 2006. A multi-scale approach to urban thermal analysis. *Remote Sensing of Environment*, 104(2), pp. 123–132.

Grouven, U., Bender, R., Ziegler, A. & Lange, S., 2007. The kappa coefficient. *Deutsche Medizinische Wochenschrift*, 132(23), pp. 65–68.

Huizhi, L., Jianguo, S., Boyin, Z., Chan, J.C.L., Cheng, A.Y.S. & Heping, L., 2002. Influences of structures on urban ventilation: A numerical experiment. *Advances in Atmospheric Sciences*, 19(6), pp. 1045–1054.

Isenburg, M., 2011. LAStools – Efficient tools for LiDAR processing. Version 111216. http://lastools.org (accessed 06 Feb. 2012).

Klysik, K. & Fortuniak, K., 1999. Temporal and spatial characteristics of the urban heat island of Łódź, Poland. *Atmospheric Environment*, 33(24–25), pp. 3885–3895.

Landis, J.R & Koch, G.G., 1977. The measurement of observer agreement for categorical data. *Biometrics*, 33(1), pp. 159–174.

Leinenkugel, P., Esch, T. & Gähler, M., 2011. Settlement detection and impervious surface estimation in the Mekong Delta using optical and SAR remote sensing data. *Remote Sensing of Environment*, 115(12), pp. 3007–3019.

Mack, B., Becker, F. & Menz, G., 2010. Mapping of impervious surfaces green vegetation fraction in urban areas using high-resolution optical and SAR data. In: *Proceedings of the ESA Living Planet Symposium*, Bergen, Norway, ESA SP-686, no pages.

Niemczynowicz, J., 1999. Urban hydrology and water management – present and future challenges. *Urban Water*, 1(1), pp. 1–14.

Oke, T.R., 1973. City size and the urban heat island. Atmospheric Environment, 7(8), pp. 769–779.

Pan, X.-Z., Zhao, Q.-G., Chen, J., Liang, Y. & Sun, B., 2008. Analyzing the variation of building density using high spatial resolution satellite images: the example of Shanghai city. *Sensors*, 8(4), pp. 2541–2550.

Priestnall, G., Jaafar, J. & Duncan, A., 2000. Extracting urban features from LiDAR digital surface models. *Computers, Environment and Urban Systems*, 24(2), pp. 65–78.

Ramanauskas, A., 2009. Entwicklung von Korrekturfaktoren zur Erfassung der innerstädtischen Versiegelung mittels HRSC-AX-Daten. Bachelor Thesis, Friedrich-Schiller-University Jena.

Richter, R., Schläpfer, D. & Müller, A., 2006. An automatic atmospheric correction algorithm for visible/NIR imagery. *International Journal of Remote Sensing*, 27(10), pp. 2077–2085.

Scalenghe, R. & Marsan, F., 2009. The anthropogenic sealing of soils in urban areas. *Landscape and Urban Planning*, 90(1), pp. 1–10.

Stehman, S.V., 1997. Selecting and interpreting measures of thematic classification accuracy. *Remote Sensing of Environment*, 62(1), pp. 77–89.

Stehman, S.V., 2009. Sampling designs for accuracy assessment of land cover. *International Journal of Remote Sensing*, 30(20), pp. 5243–5272.

Tang, Z., Engel, B.A., Lim, K.J., Pijanowski, B.C. & Harbor, J., 2005. Minimizing the impact of urbanization on long term runoff. *Journal of the American Water Resources Association,* 41(6), pp. 1347–1359.

Tucker, C.J., 1979. Red and photographic infrared linear combinations for monitoring vegetation. *Remote Sensing of Environment,* 8(2), pp. 127–150.

Xian, G. & Crane, M., 2006. An analysis of urban thermal characteristics and associated land cover in Tampa Bay and Las Vegas using Landsat satellite data. *Remote Sensing of Environment*, 104(2), pp. 147–156.

Yu, B., Liu, H., Wu, J., Hu, Y. & Zhang, L., 2010. Automated derivation of urban building density information using airborne LiDAR data and object-based method. *Landscape and Urban Planning*, 98(3–4), pp. 210–219.

Zevenbergen, L.W. & Thorne, C.R., 1987. Quantitative analysis of land surface topography. *Earth Surface Processes and Landforms*, 12(1), pp. 12–56.